40th AIAA/ASME/SAE/ASEE Joint Propulsion Conference and Exhibit
11 - 14 July 2004, Fort Lauderdale, Florida

AIAA 2004-4037

Green Rocket Propulsion by Reaction of Al and Mg Powders and Water

Timothy F. Miller* and John D. Herr†
Applied Research Laboratory, The Pennsylvania State University, State College, PA 16804

The efficacy of using aluminum-water and magnesium-water as propellants for underwater thruster applications has been investigated by the authors. The theoretical specific impulse for both reactant systems is high, and the products of reaction (alumina, magnesia, and hydrogen) are environmentally benign. The attractiveness of these systems as "green" propellants has been commented on previously, however, no practical experimentation with these systems has been made. The present work describes the testing of a linear combustor with magnesium-water and aluminum-water under conditions of pressure and oxidizer-fuel ratios and with a metal powder feed system that could be employed in actual rocket engines. Measurements of off-design specific impulse are compared with theoretical predictions that take into account two-phase losses. Measurements of heat fluxes available to vaporize regeneratively the liquid water oxidizer are presented as well. Perhaps of most importance, observations of the degree of product oxide accumulation in the combustor are presented. These measurements and observations are used to determine the effectiveness of these two metal fuel systems as practical green propellants.

Nomenclature

A_{ch}	=	cross-section area of combustor	P_{Ex}	=	exhaust plane pressure
C_p	=	specific heat of gas	P_{Ch}	=	chamber pressure
C_s	=	specific heat of condensed phase	Re	=	relative droplet Reynolds numbere
d	=	droplet diameter	R_{Gas}	=	ideal gas constant
g_c	=	1 kg-m/N-s^2	T_{Ch}	=	chamber temperature
Isp	=	specific impulse	U_{Ex}	=	exhaust plane velocity
L_{RHn}	=	length to react droplets	X	=	mole fraction
$\dot{m}$	=	mass flow rate	Y_C	=	mass fraction of condensed phases
M_i	=	molecular weight of species	τ	=	droplet/particle burn time
n	=	modified ratio of specific heat	γ	=	ratio of specific heats

I. Introduction

An interesting candidate green propellant system may employ solid powdered Al or Mg fuel and water as the oxidizer. The basic reactions are:

$$2Al + 3H_2O \rightarrow 3H_2 + Al_2O_3$$

$$Mg + H_2O \rightarrow H_2 + MgO$$

In addition to the relatively high volumetric and densimetric energy densities of these reactions, they are also desirable because the main products (alumina and magnesia) are environmentally benign. The oxidizer (water) can be easily stored, and Al powder is relatively unreactive in air. Although more reactive in air, Mg is no more dangerous to work with than many rocket propellants. Furthermore, the Mg/H_2O system may have for application as

* Senior Research Associate, Energy Science and Power Systems Division, P. O. Box 30, N. Atherton Street
† Research Associate, Energy Science and Power Systems Division, P. O. Box 30, N. Atherton Street

an in-situ produced propellant system as the Martian regolith is composed of ~8% Mg[1] and in view of the recent discoveries of water in the Martian environment.[2]

Water-breathing, solid-propellants have been considered for underwater rocket propulsion as early as the 1940s.[3]Their principal advantage is to offset the limited range of conventional solid-propellants caused by low propulsion efficiency. With one concept, the solid grain is loaded with a super-stoichiometric amount of metal (such as aluminum or magnesium) that reacts with ingested water. Specific impulse can be increased if powdered metal is used instead of the super-stoichiometric grain. Goroshin and Higgins[4] and Shafirovich et al.[5] proposed a rocket based on carbon dioxide and powdered magnesium in which a pressurized gas generator produces the powder feed. An alternative powdered fuel system was proposed by Fricke et al.[6] and Loftus et al.[7] . This method has been refined at the Applied Research Laboratory (ARL) and is suitable for high-pressure particle feed.[9] It is the system employed for the work described here.

The theoretical work of Bruno et al.[‡] advocate the use of Al/H_2O is a green propellant. Foote et al.[8] performed combustion tests on such a system at one-atmosphere pressure. Miller[10] developed a numerical model for the Al/Steam system and made predictions at elevated pressures, and obtained good agreement with Foote et al.'s low pressure data. However, no experimental work at the elevated pressures typical of rocket propulsion has been reported; nor, has any attempt to quantify the magnitude of two-phase losses that may be expected during operation. For the last several years, work has been undertaken at the ARL to study water-breathing thrusters employing powdered Mg, Al, and alloys for application underwater[11,12]. The objective of this paper is to present some of the experimental results of this work with an eye toward applications in the atmosphere or as space thrusters. The results presented here focus on more system level issues, detailed temperature and other measurements will be presented in the future. Also note that the reacting system considered here is near to stoichiometric. Therefore the solids loading of the flow is extremely high relative to previous work.

II. Theory

A. Specific Impulse

The NASA CET[13] code and an ARL modification of the SOLGAS-MIX[14] code were both used to perform initial equilibrium analyses of the reaction in the combustion chamber. These analyses predicted temperature, density, composition, and specific impulse. The CET code does not account for the effects of two-phase losses on the prediction of specific impulse. Also, we found that CET had difficulty in converging in some of the cases that were posed. Consequently, the CET calculations were supplemented by the theoretical equations described presently,[21] and by calculations made with SOLGAS-MIX.

For the case of ideal expansion with no losses, the nozzle exit velocity is calculated as:

$$U_{Ex} = \{ 2C_p T_{Ch} [1- (P_{Ex}/P_{Ch})^{(\gamma-1)/\gamma}] \}^{1/2} \quad (1)$$

with the specific impulse for a prescribed expansion ratio:

$$Isp = U_{Ex}/g_c \quad (2)$$

The specific impulse calculated by the CET code does not explicitly account for the two-phase loss effect on specific impulse. Losses result from incomplete heat transfer between the condensed phases and the gas, the ability of the condensed phase to expand, and the drag exerted by the condensed phases on the gas flow. Two limiting cases are described here.

Maximum losses occur when no heat transfer and non-accelerated particles are assumed. If the condensed phases are not accelerated, the Isp is decreased because there is a smaller amount of material exhausting at the theoretical nozzle exit velocity. The no heat transfer assumption means that there is a portion of energy stored in the condensed phase that is not available to the expanding gas. The equation for the exit velocities for the case of no heat transfer and no acceleration is the unmodified Eq. 1, however, the calculation of Isp changes:

$$Isp = (1 - Y_C) U_{Ex}/g_c \quad (3)$$

[‡] Bruno, C., Ingenito, A., and Cuoco, F., "Using Powdered Aluminum for Space Propulsion," Internet address: www.tfd.chalmers.se/~valeri/Ajax/Paper_on_Aluminum_for_Space_Propulsion.pdf, 2002.

where Y_C is the mass fraction of condensed phases. Minimum losses occur with complete heat transfer and accelerated particles. Even with this case, losses are caused by the inability of the volume occupied by the condensed phase to expand. For the case of fully accelerated particles:

$$U_{Ex}=\{2[Y_C C_S+(1-Y_C)C_p]T_{Ch}[1-(P_{Ex}/P_{Ch})^n]\}^{1/2} \quad (4)$$

where

$$n = R_{Gas}/[C_p + C_S Y_C/(1-Y_C)] \quad (5)$$

When possible, values for C_p, C_S, and R were obtained from the CET code, otherwise SOLGAS-MIX values were used. Figure 1 shows predicted Isp (for throat to exit area expansion ratio of 100) for the reaction of solid aluminum powder with liquid water and superheated steam (500 K), as well as the effects of two-phase losses. Calculations indicate a maximum theoretical Isp for the Al-steam system of @ 3200 m/s occurring at a slightly fuel lean composition. The Isp magnitude falls off only gradually with increased oxidizer. This is consistent with others' calculations. The feasibility of storing superheated steam on board seems questionable; a more practical system might store the oxidizer as liquid. Predictions of maximum theoretical Isp for a solid aluminum and liquid water system are also shown in Fig. 1 and indicate only a slight reduction in maximum Isp (@ 3000 m/s). However, for the case of the liquid oxidizer the peak value is much more pronounced. Liquid water is present in the exhaust for water/aluminum ratios greater than five. Figure 1 also shows that for the case of maximum two-phase losses, the maximum value of Isp is reduced to @ 1200 and 1700 m/s for liquid water and steam oxidizers, respectively. The water/aluminum ratio that produces this maximum is much greater than the stoichiometric ratio because the relative amount of condensed phases in the exhaust stream is reduced. The curves corresponding to minimum two-phase losses show a much more encouraging behavior (@ 2200 and 2400 m/s for liquid water and superheated steam oxidizers, respectively). Figure 2 shows similar calculations using solid magnesium powder, from which virtually identical observations can be drawn. The determination of the best powder metal fuel awaits the experimental observation of the relative and absolute two-phase loss effects.

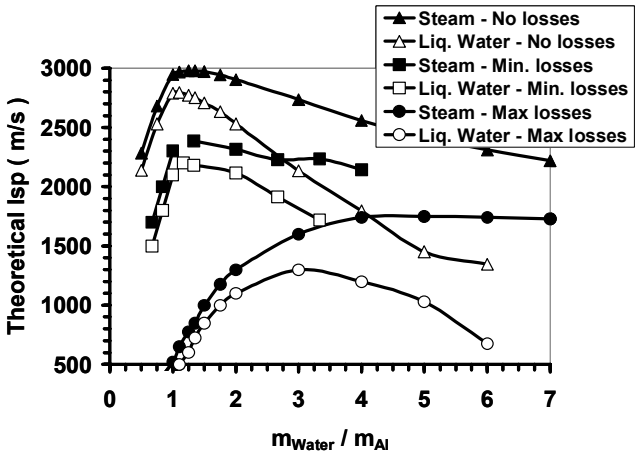

Figure 1. Theoretical specific impulse dependence on relative water flow rate for aluminum fuel.

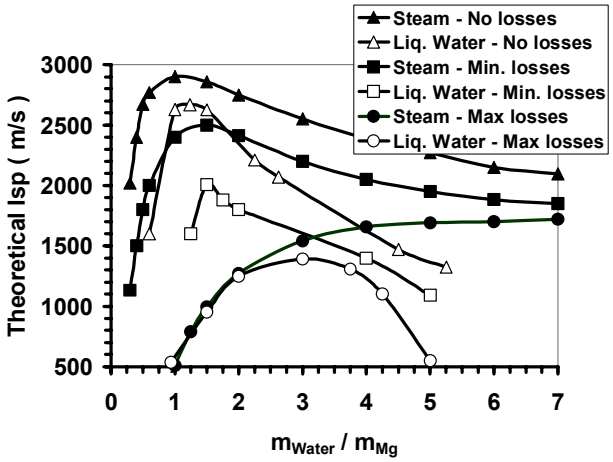

Figure 2. Theoretical specific impulse dependence on relative water flow rate for magnesium fuel.

B. Reaction Length

There is an extensive though somewhat ambiguous literature about Al and Mg particle burn times. Figure 3 shows results from a number of these references for magnesium. We have developed empirical correlations for these burn times that can be expressed as:

$$\tau/d^2=C\delta^n/[X_{OX}^{0.9}(1+.25Re^{1/2})] \quad [msec/\mu m^2] \quad (6)$$

where for Al (this correlation was originally presented in Ref. 10):

$$n = 0$$
$$C = \begin{cases} 0.15 \text{ if } P_{Ch} = 1 \text{ atm} \\ 0.075 \text{ if } P_{Ch} > 6 \text{ atm} \end{cases} \tag{7}$$

and for Mg this expression represents a simple curve fit through the data in Figure 3:

$$C = 0.007,\ n = 0 \text{ if } P_{Ch} = 1 \text{ atm} \tag{8a}$$

and

$$C = 0.02,\ n = 0 \text{ if } P_{Ch} > 4 \text{ atm} \tag{8b}$$

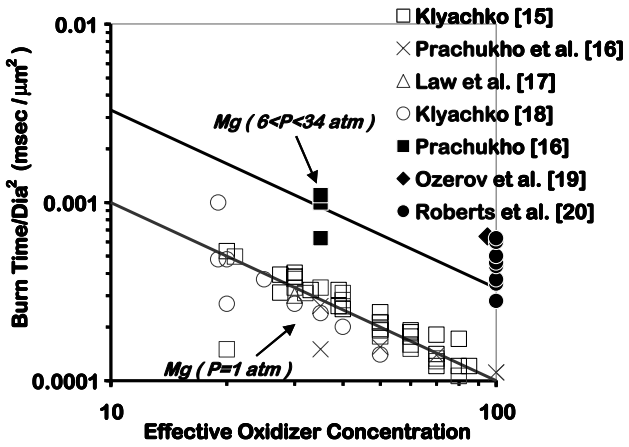

Figure 3. Burn time dependence of Al and Mg fuels on effective oxidizer concentration.

The minimum chamber length can be defined by the product of burn time and mean magnesium particle velocity in the combustion chamber. A "back of the envelope" estimate of the length required for particle reaction can be obtained by assuming that the mean particle velocity is approximately equal to the average gas velocity.[22]

$$u_m = \frac{T_{ch}\,\dot{m}_g\,R_i}{P_{ch}\,A_{ch}} \tag{9}$$

$$L_{Rxn} = \left[\frac{\tau\ T_{ch}\dot{m}_g R_i}{P_{ch}A_{ch}}\right] \tag{10}$$

In Eqs. 9 and 10, A_{ch} is the cross-sectional area of the chamber and R_i is the ideal gas constant for gas stream. The average gas velocity given by $u_{gas} = \dot{m}_g / \rho_g A_{ch}$. The burn time is given by Eq. (6).

III. Experiment

A. Fuel Feed System

As first described by Fricke et al.,[6] a fuel feed system was developed to flow powdered fuel from the storage tank to the combustion chamber. The fuel flows as a dense-phase, fluidized mixture of solid particles suspended in a carrier gas. The fuel is stored as a powder in a cylindrical pressure vessel and back-filled with a carrier gas. Upon opening a valve, the carrier gas flows from the fuel cylinder and entrains the fuel. Ideally, the amount of gas required to fluidize the fuel powder is small enough to be contained in the interstitial spaces between the fuel particles. In practice, however, a small flow rate of carrier gas is added to maintain pressure in the fuel tank. The fluidized mixture of solid fuel particles and argon gas flow through flexible fuel lines to the combustor. The lines are sized to maintain the mixture velocity above saltation, where the mixture begins to stratify. Fuel line lengths of up to 4 meters with multiple bends have not been problematic with this system. The fuel cylinder is fitted with a piston as shown in Fig. 4. A differential gas pressure is maintained across the piston during fuel flow such that the piston always contacts the fuel/gas interface. An exit orifice in the piston insures adequate gas velocity to entrain the powder. The mass ratio of fuel to carrier gas varies with the fuel but is on the order of 15:1.

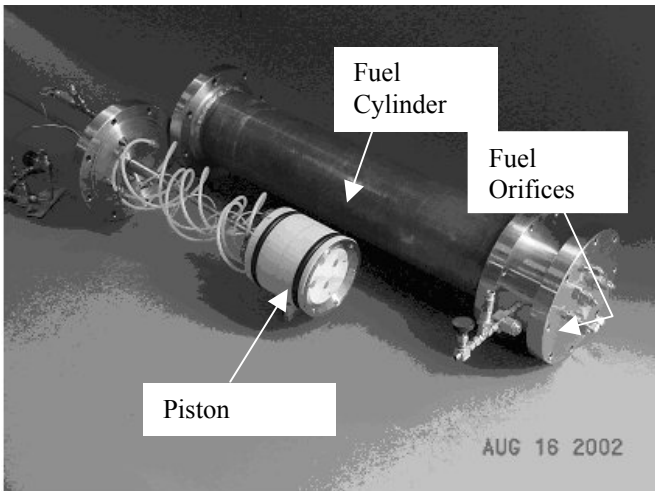

Figure 4. Photograph of powder feed assembly.

Fuel feed cylinders of 10.25, 15.25, and 17.75 cm in diameter have been tested at ARL. The largest of these fuel systems holds 59 kg of aluminum fuel and demonstrated reliable fuel flow for up to one hour. Commercial aluminum powder from one vendor with mean particle sizes of 5, 10, and 15 μm were successfully flowed with this system. A 30 μm Mg fuel from another vendor exhibited some flowability problems, but another vendor's 22 μm Mg powder demonstrated better flowability than the aluminum powders. Several fuel coatings were researched at NSWC-China Lake to optimize the flow, solids loading and packing density of powdered fuel in this system.[23]

A schematic of the fuel feed system is shown in Fig. 5. Several carrier gases have been tested with this system. Argon was selected as the carrier gas for these series of tests. In a rocket motor, an alternate carrier gas could be selected to maximize the specific impulse. The fuel system can be shut-down and restarted by opening or closing a ball valve in the fuel line (see valves 1-4 in Fig. 5). This fuel system also has throttling capabilities. At low differential pressures

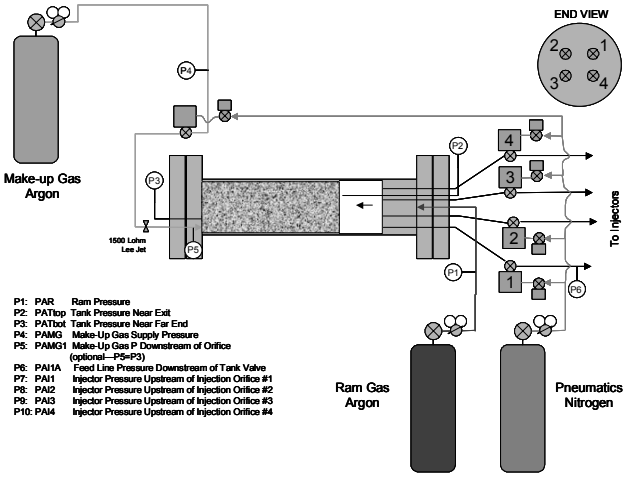

Figure 5. Schematic of powder feed system.

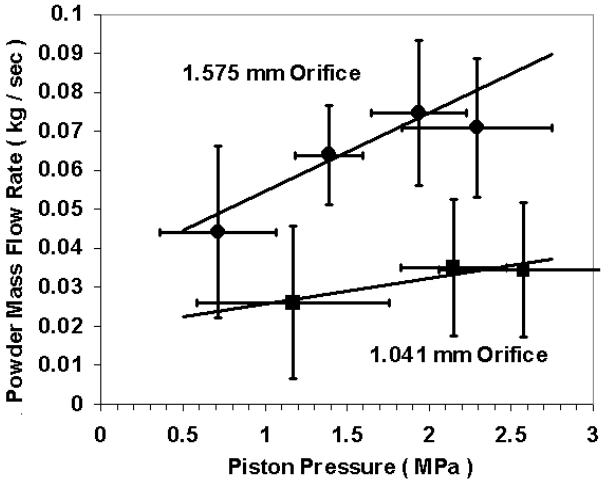

Figure 6. Powder mass flow rate control.

between the fuel storage tank and the combustor, the fuel flow follows a linear trend; at higher differential pressures, the fuel flow becomes constant.

Figure 6 shows how the powder flow rate can be controlled by varying piston pressure and orifice size. The bars denote the maximum range of instantaneous measurements made over the duration of a run. Digital throttling can also be achieved by opening or closing multiple fuel lines. In its present incarnation, the 15.24 cm and 17.8 cm diameter pistons contain four discrete orifices and fuel lines. For the series of test reported herein, one of the four lines was used for aluminum while two lines were used for the magnesium tests.

B. Combustor

The fluidized fuel and 700 K steam are premixed in a coaxial injector tube upstream of the combustor. The steam velocity is sufficiently above the saltation velocity to fluidize the fuel. The inside diameter of the combustor was 5.1 cm and the length was 0.91 m. A water jacket envelops the 1.27 cm thick graphite liners. The target equivalence ratio with either Al or Mg was 0.833 (20% excess steam). Fuel and oxidizer flowrates were adjusted to maintain a constant energy release rate in each test. The combustor was optically instrumented with six fiber optic cables leading to a spectrograph and CCD camera. Six silicon photo-detectors, and a two-wavelength pyrometer provided additional optical data at the locations shown in Fig. 7. These optical sensors were calibrated with a NIST-traceable optical standard. Combustion temperature, light intensity, ignition delay and velocity were inferred via signal processing of the above optical sensors. Figure 8 shows the instrumented combustor in the test cell.

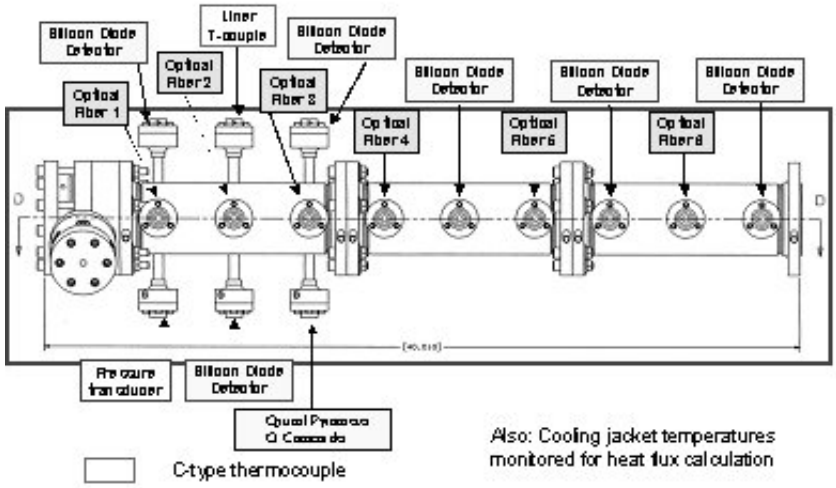

Figure 7. Sketch of combustor test assembly.

During initial testing of the combustor, a critical flow nozzle was attached to the combustor exit. At the desired operating pressure of 27 atm, the bore of this critical flow nozzle was small and tended to get obstructed with slag during aluminum fuel tests. Other interest in this project focused on expanding exhaust products through a turbine for long endurance power generation under water. Subsequently, an evaporator/slag accumulator was installed between the combustor exit and the exit nozzle as shown in Fig. 9. The evaporator contains one or more sprayers that quench the hot combustion products to about 925 K. Most of the solidified alumina fly ash exits with the hydrogen and steam, while the larger slag particles remain in the evaporator. Cooling the exhaust while evaporating water permits the use of a larger, critical flow nozzle that is less likely to clog, yet maintains the combustor pressure near 27 atm. As this combustor is scaled upwards, the

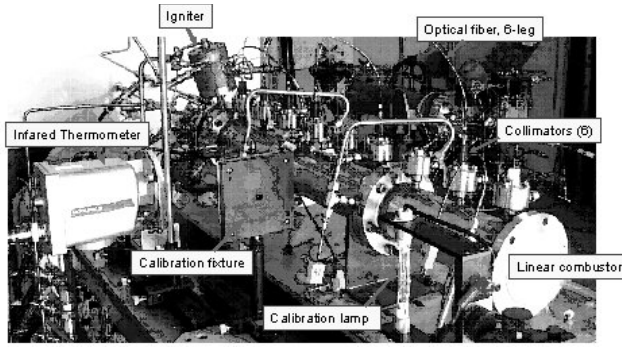

Figure 8. Photograph of combustor test assembly.

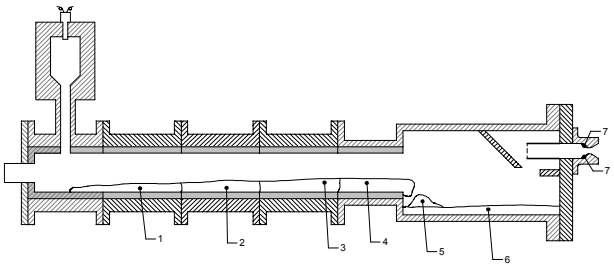

Figure 9. Sketch showing disposition of post-run alumina slag accumulation in combustor and evaporator.

nozzle throat should be sufficiently large such that a thin slag layer freezing in the nozzle will not dramatically affect operation. Pressures were measured upstream from the nozzle and also at the nozzle's throat. This permitted the two-phase pressure loss to be calculated as will be described in a following section.

Figure 10 is a photograph of the combustor in operation. The intense flare observed in the cut out in Figure 10 is produced by emission from hot alumina particles (without an evaporator/accumulator). The white vaporous exhaust from the evaporator/accumulator indicative of the addition of excess water.

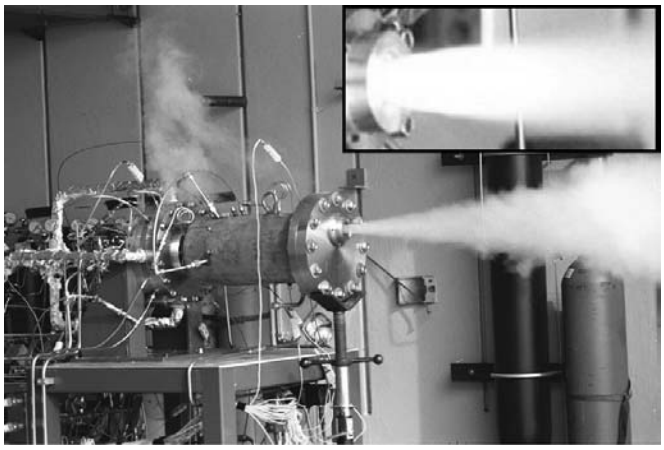

Figure 10. Combustor operation with evaporator/accumulator. Insert shows flame produced without evaporator.

C. Regenerative Cooling/Steam Generation

Steam for combustion was generated on demand in the test cell. The generator consisted of a hydrogen/oxygen combustor with controllable addition of diluent spray water. The flow-rate of water was controlled with a feedback-controlled valve to achieve the proper temperature. The total steam flow-rate was trimmed to the target value by adjusting the propellant flow rates. In a rocket application, steam for combustion could be heated by regenerative cooling of the combustor and nozzle. In our tests, the parasitic thermal power loss to the combustor walls was 71.7 kW while the thermal power required to boil and superheat water to 700 K steam for combustion was 61.2 kW. Thus, regenerative cooling appears to be a viable method of steam generation, although it was not attempted in this series of tests.

IV. Testing and Observations

Combustion was initiated with a hydrogen/oxygen torch impinging on the fluidized steam/aluminum mixture. After 35 seconds the torch was extinguished. A total of 14 tests were run with powdered metal fuels, but the nozzle throat pressure was only recorded in the five tests listed in Table I. Combustion time ranged from 95 to 635 seconds. Thermocouple, pressure transducer, and flowmeter outputs were recorded on a National Instruments data system at 500 Hz. The silicon photodetector signals were recorded at a frequency of either 500 Hz or 10 kHz; the higher data rate was used for velocity determination. The shutter on the CCD camera opened every 2.4 seconds to record simultaneous spectroscopy signals at six axial locations along the combustor thus permitting an estimation of the burn time and the length required for reaction.

Table I. Test runs used for determination of specific impulse.

Test	Run Time (s)	Fuel & Size (μm)	Fuel flow (kg/s)	Steam flow (kg/s)	P_{Ch}/P^*	Φ	Slag -free (cm)	Slag in combustor (kg)	Oxide exiting (kg)	Slag made (kg)	Excess water (kg/s)
LC7	95	Mg 30	0.0164	0.0173	1.55	.70	91	0	2.0	4.23	0.041
LC8	635	Mg 22	0.0182	0.0177	2.01	.76	91	0	0.955	19.0	0.043
LC9	215	Al 10	0.0141	0.0195	1.95	.72	5.1	1.95	0.955	5.59	0.039
LC10	95	Al 5	0.0164	0.0195	1.80	.85	7.6	0.70	1.68	2.59	0.040
LC14	95	Al[$] 5	0.0159	0.020	1.90	.80	10.2	1.07	1.5	2.41	0.042

[$] Coated w/10 % $SrMoO_4$

Table I lists the amounts of slag remaining in the various parts of the combustor and downstream collector. From these data an effective specific impulse was calculated. After each test the slag remaining in the combustor was photographed and weighed prior to cross-sectioning and analysis. When burning the 22 and 30 μm Mg powder, only a thin layer of magnesia dust remained on the

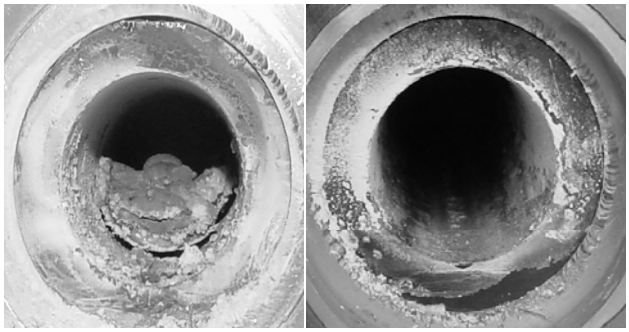

Figure 11. Post-run alumina (left) and magnesia (right) slag accumulation in combustor.

combustor walls. Conversely, a thick layer of alumina froze on the combustor walls when burning aluminum particles from 5 to 15 μm (mean). A comparison of the slag at the combustor exit is shown in Fig. 11 when burning aluminum and magnesium. The alumina slag deposited on the combustor walls from the ignition point to the combustor exit. The adiabatic flame temperature of magnesium and 700 K steam is at the freezing temperature of magnesia. If one considers the magnitude of parasitic wall heat transfer, most of the magnesia will be solidified a short distance from the burning droplet as micron-sized fly ash. That is, there is little time for any molten particles to coalesce/agglomerate before they freeze. Conversely, the measured burning temperatures for Al/steam were 2500-2600 K, which were well above the freezing temperature of alumina. Therefore, the submicron aluminum "smoke particles" as well as the larger oxide caps are molten and will tend to coalesce/agglomerate with one another and conglomerate on the combustor walls.

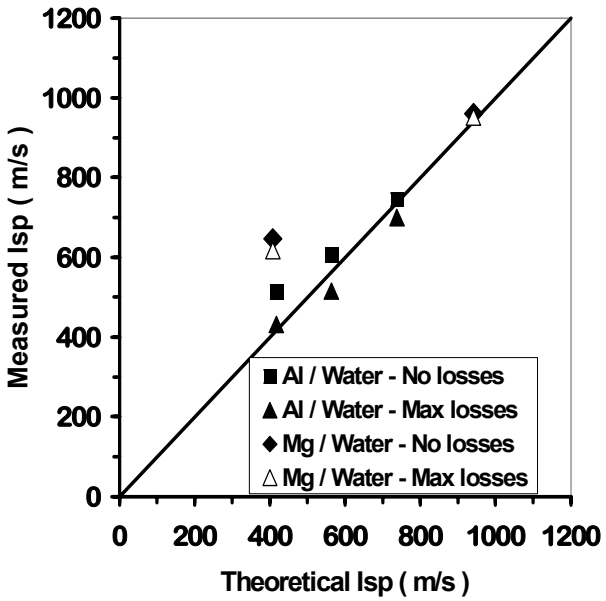

Figure 12. Comparison of theoretical and measured off-design specific impulse.

Throat pressure measurements were made in the slag accumulation chamber exit nozzle. From this measurement, the accumulation chamber pressure, the throat area, and the steam and alumina flow and accumulation rates, values for off-design specific impulse were made. These are compared with theoretical predictions assuming no, minimum, and maximum two-phase losses in Fig. 12. For Isp > 600 m/s the measured Isp agrees reasonably well with the minimum two-phase loss predictions. The poor agreement at lower Isp we attribute to the presence of liquid water in the exhaust stream.

Foote et al.[8] used the stochastic signals from two pairs of silicon photodetectors to infer a velocity in his combustor. By assuming that the bulk flow carries light perturbations downstream in the combustor, a small change in light intensity measured by one silicon photodetector will be recorded a short time later by a downstream silicon photodetector. Obviously, the perturbation must have a longer wavelength than the separation distance between the detectors, otherwise the signals have no commonality or coherence. Such long wavelength perturbations can be induced by the fuel flowrate. For example, suppose the fuel flowrate pulsates every second with a 1% change in magnitude. At the peak magnitude, the light intensity will increase as a result of the increased burning fuel cloud. As long as the time of flight, that is the separation distance between detectors divided by the velocity, is significantly less than the period of the perturbation (1 second in this example), then the downstream silicon photodetector will also record an increase in light intensity due to the flowrate perturbation. By further assuming that the flowrate perturbations are small relative to the average flowrate, then the average combustor velocity can be ascertained.

Several data sets were analyzed by performing a cross-correlation on various silicon photodetector pairs. The maxima peak (or peaks) in the correlation function indicate a maximum signal commonality which is analogous to the coherence function in the frequency domain. The number of lags at this maxima multiplied by the time between samples is the time delay. The average velocity is then calculated by dividing the axial separation distance between silicon photodetectors by the above time delay.

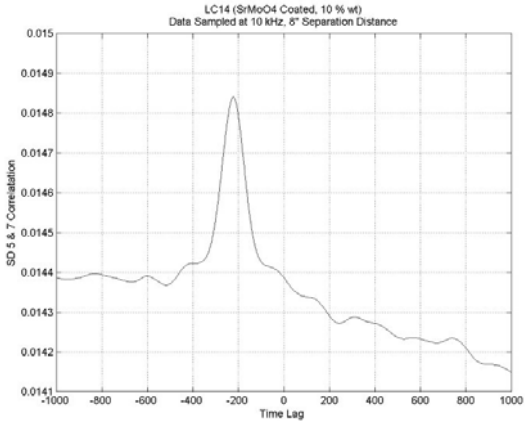

Figure 13. Photo diode intensity correlation used to infer a mean burning particle velocity.

Figure 13 shows the cross-correlation function between the silicon detectors in viewport 5 and viewport 7 during Test LC14 (an aluminum run). The maxima or greatest signal commonality occurs at lag 222.

Since the separation distance was 20.3 cm and the sampling rate was 10 kHz, the inferred velocity is 9.1 m/s. Other measurements list velocities that ranged from 9.1 to 10.1 m/s for adjacent silicon detector pairs. Similar velocities were ascertained from other tests. Bear in mind that slag deposits within the combustor liner will influence the velocity. Calculations made with Eq. 9 assuming an effective cross-section one-half the actual due to sliding, and for a predominately H_2 gas flow was 8.5 m/s. Assuming a predominately steam flow produced a velocity of 4 m/s. This suggests that a very oxidizer deprived condition exists over a substantial length of the combustor.

Figure 14 also shows flame intensity determined by use of the photo-diode array for different initial aluminum particle sizes. As expected the larger particles take longer to ignite but all of the particles are consumed within 55 cm. Figure 14 shows a comparison with aluminum and magnesium reaction lengths (for 22 μm particles) flame intensities. The magnesium takes longer to ignite, but is fully reacted in the same distance. Both Al and Mg fuels burn in a relatively short distance (from the point of view of a combustor design). The observed reaction length is compared with predictions in Fig. 15. It is interesting to note the observations of Kudryavtsev et al.[24] observed ~ 2.5x greater reaction times for aerosols of 70Fm particles reacting at high pressure, while Shushin and Dreizin[25] observed 2.5 – 3x greater reaction times for 10 – 5Fm AR particles, though no increases for Mg reacting at one atm. Because of the very dense powder flow, much of the combustion occurs in an extremely oxidizer deprived (excess H_2) configuration, thus explaining the long distance observed relative to the correlations. This is consistent with previous observations regarding particle flow velocity.

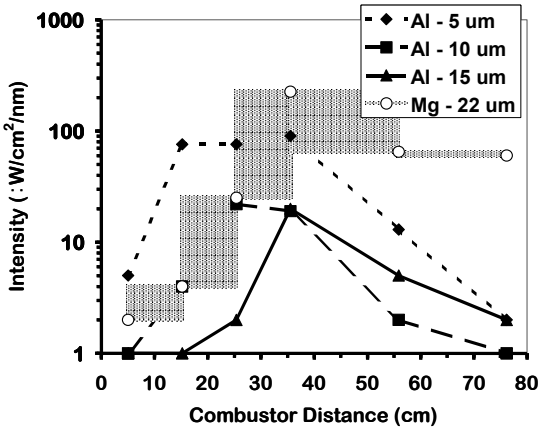

Figure 14. Comparisons of Flame Intensities for Mg and different Sized AR particles.

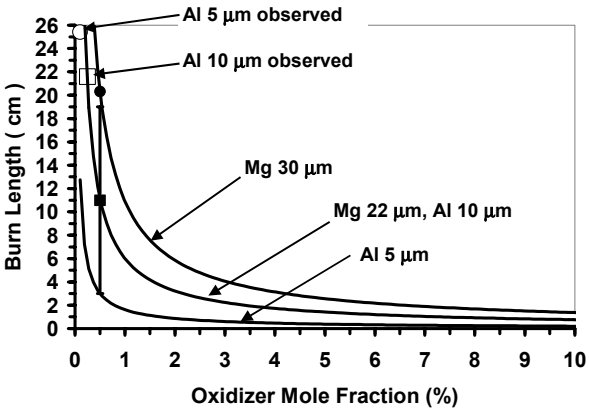

Figure 15. Comparison of theoretical and measured combustion lengths.

V. Conclusion

Aluminum and magnesium were reacted with near-stoichiometric amounts of superheated steam under conditions that closely approximate those that would be expected under rocket propulsion applications. The metal fuel was injected using a powder feed system that is also amenable for practical and throttle-capable rockets. Oxidizer steam can be generated recuperatively from heat transferred through the walls of the combustion chamber, suggesting that water oxidizer can be stored on board as a condensed phase. Sustained combustion was observed lasting up to 635 seconds. Magnesium combustion produced no slag accumulation in the combustor. Aluminum combustion produced relatively large amounts of slag accumulation, though this did not appear to compromise performance. Comparison between predictions of reaction length and observations using photodiodes indicate that the reaction length in a dense phase chamber is much longer than one would expect for solitary particles. They still indicate that a relatively short combustor can be used. A comparison of off-design (excess water) predictions and measurements of specific impulse was made in an attempt to determine the magnitude of two-phase losses. These comparisons suggest that two-phase losses can be modeled adequately by use of the minimum loss methodology. If so, this suggests that performance in the 2200-2300 m/s range for specific impulse might be expected. Clearly specific measurements of thrust and specific impulse at on-design conditions need to be undertaken.

Acknowledgments

We gratefully acknowledge the support of the Office of Naval Research via contract # N00014-00-G-0058. Kam Ng was program manager.

References

[1]Carr. M. H., *The Geology of the Terrestrial Planets*, Washington, D.C, NASA, Scientific and Technical Information Branch, 1984.

[2]Smith, M. D., "The Annual Cycle of Water Vapor on Mars as Observed by the Thermal Emission Spectrometer," *J. Geophys. Research*, Vol. 107(E11) No. 5115, 2002.

[3]Gerrard-Gough, J. D., and Christman, A.B., *History of the Naval Weapons Center, China Lake, CA, V. 2: The Grand Experiment at Inyokern*, U.S. Govt. Printing Office, Washington, D.C., 1978, pp. 298-303.

[4]Goroshin, S., and Higgins, A. J., "Powdered Magnesium-Carbon Dioxide Propulsion Concepts for Mars Missions," *35th AIAA/ASME/SAE/ASEE Joint Propulsion Conference and Exhibition*, Los Angeles, CA, 1999.

[5]Shafirovich, E. Ya., Shiryaev, A. A., and Goldshleger, U. I., "Magnesium and Carbon Dioxide: A Rocket Propellant for Mars Missions," *Journal of Propulsion and Power*, Vol. 9, No. 2, 1993, pp. 197-203.

[6]Fricke, H. D., Burr, J. W., and Sobieniak, M. G., "Fluidized Powders-A New Approach to Storable Missile Fuels," *12th JANNAF Liquid Propulsion Meeting*, CPIA Publication 201, 1970.

[7]Loftus, H. J., Montanino, and Bryndle, R. C., "Powder Rocket Feasibility Study," *AIAA/SAE 8th Joint Propulsion Specialist Conference*, New Orleans, LA, AIAA Paper 72-1162, 1972.

[8]Foote, J. P., Thompson, B. R., and Lineberry, J. T., *Combustion of Aluminum with Steam for Underwater Propulsion*, *Advances in Chem. Propulsion*, ed. G. Roy, ISBN 0-8493-1171-3, 2002.

[9]Miller, T. F., "A High-Pressure, Continuous-Operation Cyclone Separator Using a Water-Generated Flow Restriction, *Powder Technology*, Vol. 122, 2002, pp. 61-68.

[10]Miller, T. F., "Comparisons of Simulation and Experiment in a Linear Al/Steam Combustor," *36th JANNAF Combustion Meeting*, Cocoa Beach, FL, 1999.

[11]Stinebring, D. R., Cook R. B., Dzielski J. E., Kunz, R. F., and Miller, T. F., "High-speed Supercavitating Vehicles," *Applied Research Laboratory Review 2000*, pp. 31-38, The Pennsylvania State University, 2001.

[12]Miller, T. F., Walter, J. L., and Kiely, D. H., "A Next-Generation AUV energy System Based on Aluminum-Seawater Combustion," *Proc. 2002 Workshop on Autonomous Underwater Vehicles* (AUV '02 sponsored by OES/IEEE), San Antonio, TX, AIAA Paper 02-3788, Jun. 2002.

[13]NASA Lewis Research Center, "Computer Program for Calculation of Complex Chemical Equilibrium Composition, Rocket Performance, Incident and Reflected Shocks, and Chapman-Jouguet Detonations," National Aeronautics and Space Administration, 1976.

[14]Peters, J. A., "Development of a Database of Thermochemical Parameters for Use with the SOLGASMIX Computer Program," ARL Tech. Report TR 88-008, 1988.

[15] Klyachko, L. A., "Combustion of a Stationary Particle of Low-Boiling Metal," *Combustion, Explosion, and Shock Waves*, Vol. 7, 1971, pp. 199-202.

[16]Prachukho, V. P., Ozerov, E. S., and Yurinov, A. A., "Burning of Magnesium Particles in Water Vapor," *Combustion, Explosion, and Shock Waves,*, Vol. 7, 1971, pp. 195-198.

[17]Law, C. K., and Williams, F. A., "Combustion of Magnesium Particles in Oxygen-Inert Atmospheres," *Combustion and Flame*, Vol. 23, 1967, pp. 173-182.

[18]Klyachko, L. A., "Combustion of a Stationary Particle of Low-Boiling Metal," *Combustion, Explosion, and Shock Waves*, Vol. 5, 1969, pp. 279-284.

[19]Ozerov, E. S., and Yurinov, A. A., *Combustion, Explosion, and Shock Waves*, Vol. 13, 1977, pp. 778-780.

[20]Roberts, T. A., Burton, R.L., and Krier, H., "Ignition and Combustion of Aluminum/Magnesium Alloy Particles in O_2 at High Pressure," *Combustion and Flame*, Vol. 92, 1993, pp. 125-143.

[21]Hill, P. G. and Peterson, C. R., *Mechanics and Thermodynamics of Propulsion*, Reading, MA: Addison-Wesley Publishing Company, 1965.

[22]Linnell, J. A. and Miller, T. F., "A Preliminary Design of a Magnesium Fueled Martian Ramjet Engine," *AIAA/ASME/SAE/ASEE 38th Joint Propulsion Conference*, Indianapolis, IN, AIAA Paper 02-3788, 2002.

[23]Sullivan, R. M., Johnson, C. E., and Higa, K. T. "Improving the Flowability of Metal Powders," Naval Air Warfare Center Weapons Division, NAWCCWD TP 8573, China Lake, CA, Feb. 2004.

[24]Kudryavtsev, V. M., Sukhov, A. V., Voronetskii, A. V., and Shpara, A. P., "High-Pressure Combustion of Metals (Three-Zone Model)," *Combustion, Explosion, and Shock Waves*, Vol. 15, 1979, pp. 2239-2247.

[25]Shoshin, Y., Dreizin, E., "Particle Combustion Rates in Premixed Flames of Polydisperse Metal-Air Aerosols," *Combustion and Flame*, Vol. 133, 2003, pp. 275-287.